Check for updates

Batteries & Supercaps

Research Article
doi.org/10.1002/batt.202400365

Chemistry Europe
European Chemical Societies Publishing

www.batteries-supercaps.org

Aqueous Acidic Pectin-Based Solution as Electrolyte and Pretreatment Solution for Zinc Ion Battery Anodes

Jooyoung Jang,[a] Won-Gwang Lim,[b] and Changshin Jo*[a, c]

While considerable progress has been achieved in aqueous mildly acidic Zn-ion batteries (AZIBs), the development of metallic Zn anodes remains challenging due to dendritic growth and side reactions on the Zn surface in mildly acidic aqueous environments. Herein, we utilize pectin in two ways: firstly, as an additive for the acidic $ZnSO_4$ electrolyte with pectin (referred to as ZSP); and secondly, as a component in the pretreatment solution for Zn electrode. The ZSP electrolyte can prevent the formation of inactive $Zn_4(OH)_6(SO_4)\cdot 5H_2O$ byproduct on Zn electrode and enable stable cycling under challenging conditions at 10 mA h cm^{-2}. Interestingly, the immersion of the Zn foil in the acidic pectin solution resulted in the uniform removal of the bumpy oxides/carbonates layer on the Zn metal surface. The cells with treated Zn electrode in pectin solution exhibited lower overpotentials and effectively inhibited cell failure. Our findings indicate that utilizing an organic-based acidic $ZnSO_4$ electrolyte shows promise as both an effective electrolyte and a pretreatment solution for the development of stable and cheap aqueous AZIB electrolytes.

1. Introduction

Mildly acidic aqueous Zn-ion batteries (AZIBs) have attracted great attention due to their inherent safety, cost-effectiveness, and higher ionic conductivity resulting from the use of aqueous electrolytes compared to nonaqueous electrolyte systems.[1] Metallic Zn foil, anode in AZIBs, is promising material because of natural abundance and good compatibility with aqueous media compared to other metallic anodes (e.g., Li, Na, and K, etc.).[2] Moreover, Zn metal has high gravimetric and volumetric capacities (820 mA h g^{-1} and 5855 mA h cm^{-3}), and low redox potential (−0.78 V vs. standard hydrogen electrode). However, Zn metal suffers from the formation and growth of dendritic Zn during cycling and exhibits poor plating/stripping reversibility which hampers AZIBs to be commercialized as next-generation battery systems.[3]

According to the thermodynamic principles of the Pourbaix diagram for Zn, the potential of hydrogen (pH) of electrolyte solution has a significant impact on Zn electrode surface and the Zn plating/stripping process.[2a,4] In alkaline environments, Zn electrodes tend to passivate due to the formation of the insulating byproducts such as ZnO and $Zn(OH)_2$.[5] On the other hand, recent research showed highly improved reversibility with minimized byproduct formation can be achieved by using neutral or mildly acidic aqueous electrolytes (e.g., 1 M $ZnSO_4$, denoted as ZS).[2a,6]

However, challenges arise due to the unavoidable hydrogen evolution reaction (HER) when H_2O/H^+ directly contacts with Zn surface because of the lower redox potential of Zn^{2+}/Zn than onset potential of the HER.[7] As a result of the HER, the local concentration of OH^- ions on the Zn electrode surface increases, leading to an irreversible increase in pH values. As the cycling prolongs, the pH value rises steadily, and hydroxide ions react with Zn^{2+}, H_2O, and SO_4^{2-} to form the porous Zn hydroxide and inactive Zinc hydroxide sulfate (ZHS, $Zn_4(OH)_6(SO_4)\cdot 5H_2O$) byproducts, leading to the continuous accumulation of inactive layer on the Zn surface.[8] In our preliminary experiment, after immersing the Zn anode in ZS electrolyte for two days, we observed chemically formed ZHS through the scanning electron microscopy (SEM) images and X-ray diffraction (XRD) pattern, consistent with reported results in literature (Figures S1, S2).[8a,9] Furthermore, in Zn symmetric and Zn||Cu asymmetric configuration cells using Zn electrodes that were soaked in ZS electrolyte, the polarization increased compared to the cells with pristine Zn (Figure S3). This indicates that ZHS agglomerates act as a physical barrier that hinders the transfer of electrons and ions at the electrode-electrolyte interface, leading to an increase in the internal resistance.[8a,10] Additionally, excessive ZHS formation may lead to repetitive loss of both $ZnSO_4$ salt and H_2O molecules, causing partial crystallization of salt after long-term cycling.[5c,11]

To tackle these challenges, various strategies involving advanced electrolytes with organic/inorganic additives[12] and hybrid electrolytes[13] containing organic solvents have been explored. Recently, studies have explored the use of monomeric organic acids to suppress the formation of the passivation layer and maintain a stable pH environment in aqueous electrolytes, thereby improving the reversibility of Zn anodes. Zeng et al.

[a] J. Jang, C. Jo
Graduate Institute of Ferrous & Eco Materials Technology (GIFT), Pohang University of Science and Technology (POSTECH), 77 Cheongam-Ro, Nam-Gu, 37673 Pohang, Gyeongbuk, Republic of Korea

[b] W.-G. Lim
Department of Chemical and Biomolecular Engineering, Korea Advanced Institute of Science and Technology (KAIST), 291 Daehak-Ro, Yuseong-Gu, 34141 Daejeon, Republic of Korea

[c] C. Jo
Department of Chemical Engineering, Pohang University of Science and Technology (POSTECH), 77 Cheongam-Ro, Nam-Gu, Pohang 37673, Gyeongbuk, Republic of Korea
E-mail: jochangshin@postech.ac.kr

Supporting information for this article is available on the WWW under https://doi.org/10.1002/batt.202400365

© 2024 Wiley-VCH GmbH

Research Article
doi.org/10.1002/batt.202400365
Chemistry Europe
European Chemical Societies Publishing

achieved long-term cyclability of Zn anode by adding sulfuric acid (H_2SO_4) to a 3 M $ZnSO_4$ electrolyte, adjusting the pH value of the electrolyte to 1.85.[14] The lifespan of a Zn symmetric cell with modified electrolyte was extended by approximately three times compared to that of the cell with the pure electrolyte. This improvement can be attributed to alleviated dendrite formation and effectively addressed local OH^- formation issue. As another example, Pan group produced an acidic $Zn(CF_3SO_3)_2$ electrolyte (pH~1.6) by introducing tetramethylene sulfone and a trace amount of acetic acid as buffering agent.[15] They also observed a significant improvement in cycle stability under acidic environment compared to the case where only the buffering agent was used. However, while some studies have claimed the effectiveness of acidic electrolytes with additives in AZIBs, their effect on the mitigation of side reactions and electrode surface modification has been poorly understood.

On the other hand, acidic solutions have also been used as pretreatment solutions for the Zn anode surface.[16] Wang et al. produced a porous Zn structure by immersing metallic Zn in the acidic solution of trifluoromethanesulfonic acid (TFA) with acetonitrile (AN) for 24 h.[17] The dissociated proton in the TFA-AN solution reacts with metallic Zn, resulting in the production of hydrogen and the formation of the porous structure. The results of this study imply that the acidic electrolytes containing additives mentioned in literature can induce chemical reactions on the surface of Zn foil. We also performed a verification test, when the Zn metal was immersed in ZS containing H_2SO_4 with a pH value of 2.07 for two days, the bumpy surface of Zn foil was etched away and corrosion reaction occurred, forming numerous pits (Figure S4). As confirmed in our test, acidic electrolytes lead to surface corrosion due to excessive HER on Zn metal, while also having the potential as a solution for surface modification by etching away uneven layers on the surface.

In this study, we examined the effect of biopolymer on Zn metal surface. Biopolymers have demonstrated several advantages in battery systems where they are employed as separators,[18] binders,[19] and hydrogel electrolytes.[20] Biopolymers are stable in acidic environment and lower the pH of aqueous electrolyte.[21] Specifically, carboxyl groups, abundant in biopolymers, can release hydrogen ions (H^+) in aqueous solution, forming carboxylate groups, which make electrolyte acidic.[22]

Among the biopolymers, pectin was used as an electrolyte additive in the ZS electrolyte (Figure 1a). With 5 wt% of pectin in ZS (1 M ZS with 5 wt% of pectin, ZSP) electrolyte, having a low pH value of 2.04, the ZHS formation and the surface corrosion are effectively suppressed compared to ZS electrolyte with H_2SO_4 at the same pH level. Moreover, it is noteworthy that Zn||Cu cell with ZSP electrolyte maintained stable operation for approximately 23 times and 12 times longer compared to cells with ZS at high-capacity conditions with 1 mA h cm^{-2} and 4 mA h cm^{-2}, respectively. Notably, we also observed that the pectin solution as pretreatment solution uniformly etched the bumpy layer on the surface of Zn electrode. The surface-modified Zn anode with ZSP (Zn@ZSP) not only improves wettability to aqueous media but also

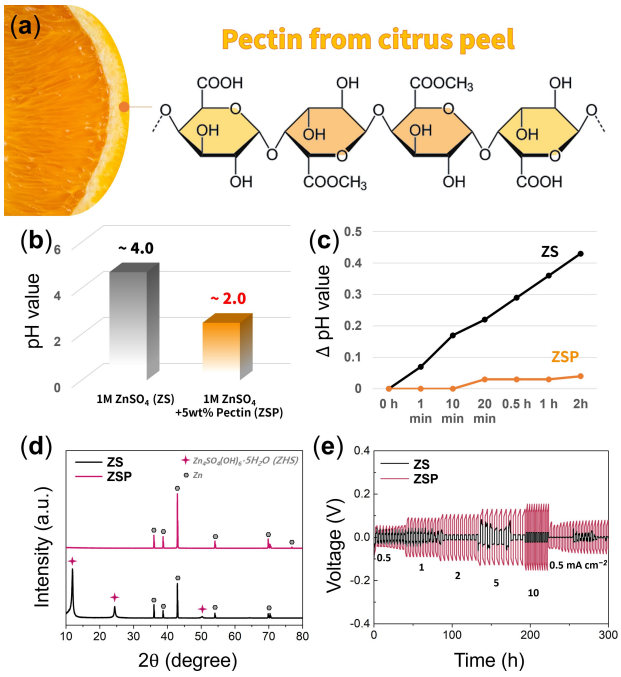

Figure 1. a) Illustration of chemical structure of pectin. b) The pH values of 1 M $ZnSO_4$ (ZS) and 1 M $ZnSO_4$ with 5 wt% pectin (ZSP). c) The pH value changes when Zn metals was immersed in 15 mL of ZS and ZSP solutions. d) XRD peaks of Zn electrodes immersed in the ZS and ZSP electrolytes for two days. e) Voltage profiles of Zn symmetric cell cells with ZS and ZSP electrolytes with capacity of 1 mA h cm^{-2} with different current densities.

reduces internal resistance and charge transfer resistance. The full cells using V_2O_5 and MnO_2 cathodes with Zn@ZSP exhibited reduced internal resistance and improved cycle stability without failure compared to Zn soaked in the ZS electrolyte. This study will also serve as a point of reference for AZIBS with acidic electrolyte, which introduces various types of organic acids as additives.

2. Results and Discussion

2.1. Acidic $ZnSO_4$ Electrolyte with Pectin for AZIBs

Pectin is a complex acidic polysaccharide found in plant cell walls in fruits and is commercially used as a thickening and gelling agent due to its ability to bind water.[23] The chemical structure of pectin, rich in D-galacturonic acid units, features an open form with an aldehyde group (–CHO) at C1, hydroxyl groups (–OH), and a carboxylic acid group (–COOH) at C6 (Figure 1a).[24] In particular, the carboxyl groups in pectin can ionize in water, effectively lowering the pH value of the aqueous solution.[25]

The pH value of the electrolyte upon pectin addition was measured using a pH meter. We observed a significant decrease in pH value with increasing pectin content, confirming that pectin made the electrolyte more acidic (Figure 1b). When Zn metal disk with a diameter of 16 mm was immersed in ZS electrolyte, the pH value changed dramatically despite the

© 2024 Wiley-VCH GmbH

25666223, 2024, 12, Downloaded from https://chemistry-europe.onlinelibrary.wiley.com/doi/10.1002/batt.202400365 by University of Ulsan, Wiley Online Library on [11/11/2025]. See the Terms and Conditions (https://onlinelibrary.wiley.com/terms-and-conditions) on Wiley Online Library for rules of use; OA articles are governed by the applicable Creative Commons License

solution being excessive. This indicates the occurrence of a water decomposition reaction and formation of hydroxide ions on the surface of Zn metal, with byproducts such as ZHS possibly being formed. On the other hand, the ZSP solution showed almost no pH change. This indicated that the pectin could act as buffering agent retain a stable pH environment in the aqueous Zn electrolytes. The oxygen-containing functional groups in pectin may form hydrogen bonds with water molecules,[26] which could lower water activity and inhibit changes in the pH value of the solution (Figure 1c).[15] We tested Zn||Cu cells using 1 M $ZnSO_4$ (ZS) with different pectin concentrations at 2 mA cm^{-2} with an areal capacity of 4 mA h cm^{-2} to investigate the effect of acidic pectin-based electrolyte in AZIBs (Figure S5). The introduction of 0.5 and 1.5 wt% pectin into the ZS electrolytes led to a decrease in initial coulombic efficiency (ICE) and an increase in polarization overpotential as depicted in Figures S6a, b. Nevertheless, with the increase in pectin concentration, there was a tendency for ICE to increase, leading to an improvement in cycle life. Based on the results, we selected 1 M ZS with 5 wt% of pectin (ZSP) with ~2 of pH value as the optimized pectin content because the cell with ZSP exhibited highest cycle stability for >800 h under harsh condition of 4 mA h cm^{-2} with 99.7% of average CE compared to that of ZS (short circuit after 60 h). Even when compared to the cycling performance of Zn||Cu cell with 1 M $Zn(CF_3SO_3)_2$ electrolyte, which has been actively applied in previous AZIBs' research and known for mitigating byproduct formation, the Zn||Cu cell with ZSP demonstrated better stability (Figure S7).[27]

As mentioned in the introduction part, the X-ray diffraction (XRD) peaks revealed the presence of ZHS on the Zn electrode after it had been immersed in the ZS electrolyte for two days. Contrary to the results of the ZS electrolyte, the XRD peaks of ZHS on the Zn metal immersed in the ZSP electrolyte were not observed (Figure 1d). The lower bulk pH of the ZSP has the potential to inhibit the increase of local pH on the surface, leading to the suppression of ZHS formation.

The electrochemical properties between the cells using ZS and the ZSP electrolytes were comparatively investigated. First, the solution resistances (R_S) were determined from electrochemical impedance spectroscopy (EIS) spectra of titanium (Ti) symmetric cells using ZS and ZSP. The R_S values of ZS and ZSP are 0.99 and 0.86 ohm, respectively, which correspond to the ionic conductivity of 13.17 and 15.13 mS cm^{-1}, respectively (Figure S8). There is no significant difference in ionic conductivity despite the increased viscosity by the addition of pectin, which is a high-molecular-weight carbohydrate polymer. Density functional theory and molecular dynamics simulations results showed that carboxylate and carboxyl groups cause a strong charge interaction with Zn^{2+} and induce the fast transport of Zn^{2+} ions.[20c,26c] Due to pectin, which is rich in carboxylate and carboxyl groups, ionic conductivity may not be significantly different from ZS electrolyte.

Additionally, the carboxyl groups of pectin can form hydrogen bonds with water molecules, which can increase the oxygen evolution reaction (OER) potential.[28] Through the linear sweep voltammetry tests of Zn||Ti cells, we confirmed the OER potential of the cell slightly increased with the introduction of pectin (Figure S9). Moreover, under rate performance test, ZSP-based Zn symmetric cell exhibited stable cycling performance even under high current density of 10 mA cm^{-2}, exhibiting an impressive average CE of 99.97%. However, the Zn symmetric cell with ZS electrolyte experienced failure at 1 mA cm^{-2}, making it difficult to determine the exact CE values. These results highlight the enhanced reversibility and durability of the Zn electrode in the pectin-based electrolyte (Figures 1e, S10).[29]

The first process in AZIBs operation involves the discharge reaction, stripping reaction in Zn electrode. If the morphology of Zn surface after first stripping process exhibits uneven and bumpy structures, it can accelerate the growth of dendritic Zn.[30] Therefore, the morphology of the stripped Zn anode has a profound effect on the subsequent charging process.[31] To investigate the stripping behavior of the Zn surface with electrolytes, the Zn||Cu cells were discharged at 2 mA cm^{-2} with 2 mA h cm^{-2}. SEM images of the Zn anode in the ZS electrolyte after the first stripping process revealed an uneven and rough morphology with messy small particles (Figure 2a). In contrast, the Zn electrode in ZSP displayed a cleanly stripped morphology (Figure 2b). The results demonstrated that the Zn electrode can be neatly stripped without Zn particulates in the ZSP electrolyte, revealing the intrinsic interior of the Zn electrode. Furthermore, macroscopic SEM images showed that, in contrast to the Zn electrode in ZS, the Zn electrode in ZSP electrolyte uniformly engages in the stripping reaction across a substantial area, on the order of the millimeter scale (Figure S11).

Before observing the subsequent Zn deposition morphology on the Zn electrode following the initial stripping process, the results of chronoamperometry (CA) tests can offer an understanding of the nucleation and diffusion behavior about dendritic Zn growth.[32] The significant change in current in the Zn symmetric cell with ZS at a constant potential of −150 mV signifies an increase in the surface area according to the Cottrell equation,[33] indicating accelerated the localized growth of dendritic Zn structures (Figures 2c and d bottom). In contrast, the current value in the cell containing ZSP remained relatively constant over the same duration, implying improved uniformity of Zn nucleation sites and enabling homogeneous Zn deposition (Figures 2c, d top). Additionally, the effect of the ZSP on the anode corrosion can be explored via linear polarization measurement (Figure 2e). Compared to the Zn anode in ZS electrolyte, the corrosion potential of Zn anode in ZSP shifted positively from −1.009 V to −0.989 V and the corrosion current greatly reduced from the 1.06 mA cm^{-2} to 0.57 mA cm^{-2}, confirming the improved the corrosion resistance of Zn anode in ZSP electrolyte.[12b,34] Furthermore, the contact angle of the ZSP electrolyte (70°) was smaller than that of the ZS electrolyte (99°) (Figure 2f). This indicates that the ZSP electrolyte provided sufficient hydrophilicity to the Zn electrode, effectively enhancing the affinity between the electrolyte and electrode.[35] It has been widely reported that the strong affinity between the Zn electrode and the electrolyte due to the enhanced hydrophilicity effectively inhibits dendritic Zn growth.[31,36]

© 2024 Wiley-VCH GmbH

25666223, 2024, 12, Downloaded from https://chemistry-europe.onlinelibrary.wiley.com/doi/10.1002/batt.202400365 by University of Ulsan, Wiley Online Library on [11/11/2025]. See the Terms and Conditions (https://onlinelibrary.wiley.com/terms-and-conditions) on Wiley Online Library for rules of use; OA articles are governed by the applicable Creative Commons License

Research Article
doi.org/10.1002/batt.202400365
Chemistry Europe
European Chemical Societies Publishing

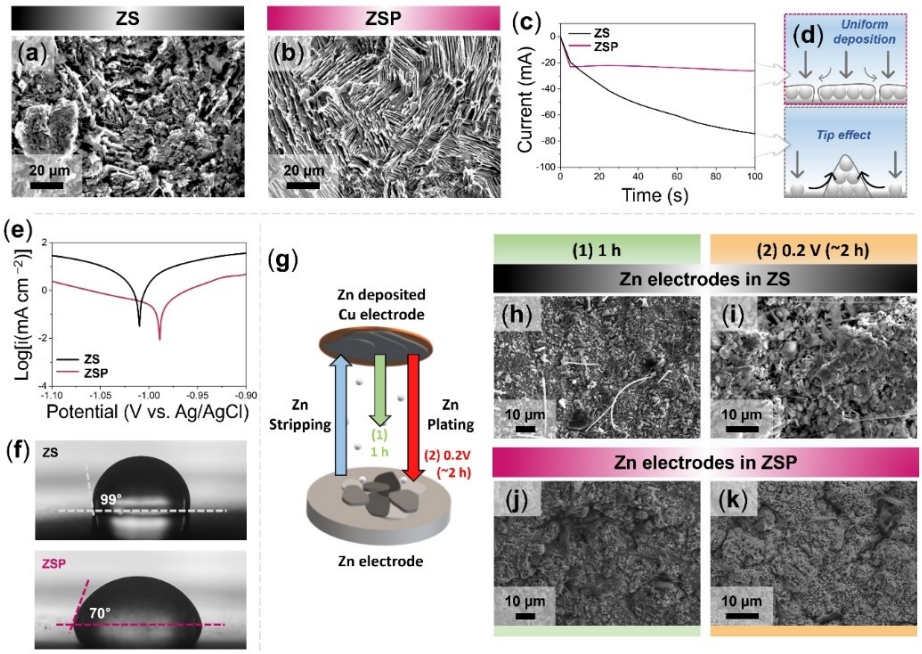

Figure 2. SEM images of Zn electrode after stripping process with a) ZS and b) ZSP electrolytes. c) Chronoamperometry test results of Zn symmetric cell with ZS and ZSP electrolyte. d) Schematic diagram of uneven Zn deposition caused by the tip effect in ZS electrolyte (bottom) compared to uniform Zn deposition in ZSP electrolyte (top). e) Linear polarization curves of ZS and ZSP electrolytes. f) The contact angles of the droplets of ZS (top) and ZSP (bottom) electrolytes on bare Zn. g) Schematic diagram of Zn||Cu cell test method for SEM analysis. The SEM images of Zn electrodes depending on deposition time with h–i) ZS and i–k) ZSP electrolytes.

To visually verify the deposition morphology following the initial Zn stripping at 2 mA cm^{-2} with 4 mA h cm^{-2}, Zn was deposited onto the stripped Zn electrode by varying the deposition time (Figure 2g). When examined after deposition at 2 mA cm^{-2} for one hour, the Zn electrode's surface in ZS was covered with irregular flake-like dendrite agglomerates and lumpy byproducts (Figure 2h). Further deposition up to 0.2 V (~2 h) resulted in agglomerated structure, indicating uncontrolled Zn deposition (Figure 2i). On the other hand, in the Zn electrode with ZSP, Zn was evenly deposited over a large area without huge Zn agglomerates, thanks to the formation of uniform nucleation sites, which is consistent with the results obtained from CA test (Figures 2j, k).[37]

In AZIBs, the use of glass fiber membrane (GFM) separator presents challenges due to its fragile nature during deep cycling (>4 mA h cm^{-2}).[38] The broken and separated fibers can create isolated Zn fragments, referred to as dead Zn, thereby reducing the reversibility of Zn stripping/plating behavior. In the Zn||Cu cell with ZS after five cycles at 2 mA cm^{-2} with 4 mA h cm^{-2}, the Zn deposition morphology on Zn anode appeared bumpy and intertwined with the fibers pulled down from the GFM (Figure S12). The glass fibers have high binding energies (−2.26 eV) with Zn metal, causing numerous Zn dendrites to penetrate the GFM, and the broken fibers are intermingled with deposited Zn.[39] As previously noted, the high-molecular-weight carbohydrate polymer, pectin, can fill the inner space of the GFM membrane with a matrix in ZSP, thereby suppressing fiber breakage.[40] Thus, Zn was uniformly deposited in the cell with ZSP, and the pectin electrolyte inhibited the agglomeration between glass fibers and isolated Zn fragments under the same conditions (Figure S13).[41]

Figure S14a–c demonstrated the ex situ XRD patterns of Zn electrode obtained from Zn||Cu cells. The cells experienced an aging process for 12 hours, followed by a discharge process (Zn stripping from Zn anode) for 2 h, and then a charge process (Zn deposition on Zn anode) to 0.2 V at 2 mA cm^{-2} (Figure S14a). The XRD result of the Zn electrode from a Zn||Cu cell with ZS aged for 12 hours showed a pattern corresponding to ZHS byproducts (purple box in Figure S14b).[42] Moreover, the presence of ZHS on the Zn electrode surface can be also observed by the characteristic peaks of ZHS during the discharge and charge process. Additionally, we observed that during the Zn deposition process on the Zn anode, the intensity of the (002) peak of the Zn electrode increases, while the intensity of the ZHS peak decreases and the orientation of ZHS changes.[43] This may be due to the ZHS being covered as Zn is deposited.

In contrast, in the case of the Zn electrodes from Zn||Cu cells with ZSP, there are no XRD patterns corresponding to ZHS byproduct (Figure S14c). These results support the effectiveness of the ZSP electrolyte in suppressing the formation of ZHS byproducts during the aging and charge-discharge processes.

2.2. Pectin Solution for Surface Pretreatment

Previous studies have demonstrated the ability of acidic solutions to etch and modify metallic Zn surfaces.[16a,17,44] We

© 2024 Wiley-VCH GmbH

25666223, 2024, 12, Downloaded from https://chemistry-europe.onlinelibrary.wiley.com/doi/10.1002/batt.202400365 by University of Ulsan, Wiley Online Library on [11/11/2025]. See the Terms and Conditions (https://onlinelibrary.wiley.com/terms-and-conditions) on Wiley Online Library for rules of use; OA articles are governed by the applicable Creative Commons License

Research Article
doi.org/10.1002/batt.202400365
Chemistry Europe
European Chemical Societies Publishing

25666223, 2024, 12, Downloaded from https://chemistry-europe.onlinelibrary.wiley.com/doi/10.1002/batt.202400365 by University of Ulsan, Wiley Online Library on [11/11/2025]. See the Terms and Conditions (https://onlinelibrary.wiley.com/terms-and-conditions) on Wiley Online Library for rules of use; OA articles are governed by the applicable Creative Commons License

investigated the role of the pectin-based electrolyte as a surface pretreatment solution, adjusting its acidity with a pH value of 2.0. To examine the change in surface morphology of Zn electrode resulting from electrolytes immersion, the metal, prepared by cutting a circular disk with a diameter of 16 mm, was submerged in the electrolytes for two days. Zn electrodes immersed in ZS and ZSP are denoted as Zn@ZS and Zn@ZSP, respectively. In the case of Zn@ZS, the ZHS agglomerates were formed even with a small amount of electrolyte (100 μL) (Figure 3a). Furthermore, energy dispersive spectroscopy (EDS) mapping images revealed distinct color distributions of Zn and S elements within the bulky agglomerates, providing clear evidence of ZHS formation (Figure 3a inset). For the Zn@ZSP case, the ZHS formation was effectively suppressed (Figure 3b). Additionally, X-ray photoelectron spectroscopy results revealed that the spectra of the surface of Zn@ZSP electrode did not exhibit S 2p peaks, in contrast to the Zn@ZS surface, confirming the preventive effect in ZHS formation (Figure 3c).[45]

To clarify the effect of acidic pectin solution on the Zn foil surface, metallic Zn foil was immersed in an excessive electrolyte (10 mL). In the ZS electrolyte, ZHS particles with a size range of 20–50 μm were observed on the surface (Figure 3d); whereas, in the pectin solution, no discernible ZHS formed (Figures 3e, S15). Furthermore. the bumpy layer on the Zn electrode was removed and Zn@ZSP foil clearly revealed the clean polycrystalline nature of the Zn metal.

To examine the influence of pretreatment solutions with varying pectin concentrations, we analyzed the surface morphology of treated Zn foils immersed in solutions containing different mass fractions of pectin, adjusted according to the amount of $ZnSO_4$ salt. Prior to immersion, we measured the pH values of these solutions and observed a significant decrease in pH value with increasing pectin content, indicating acidification of the solutions (Figure S16). Specifically, the pH value of 0.5 wt% and 1.5 wt% pectin solution decreased significantly compared to that of the ZS electrolyte, then stabilized around 2 in 5 wt% to 10 wt% pectin solution.

Subsequently, we examined the surface morphology of Zn electrode immersed the pectin-based solution for two days (Figure S17). When Zn foil was immersed in a 0.5 wt% pectin solution, we observed the formation of minor ZHS byproducts on the Zn surface. Adding 1.5 wt% or more pectin prevented the formation of byproducts, revealing grain boundaries of polycrystalline Zn. However, in 7.5 wt% and 10 wt% pectin solutions, excessive etching occurred, resulting some pits on the surface.

Revisiting the results of the acidic electrolyte, as explained in the introduction part, we adjusted the pH value of the ZS electrolyte to be similar to ZSP by adding H_2SO_4 (referred to as ZS-H_2SO_4 electrolyte). The immersed Zn metal in the ZS-H_2SO_4 solution exhibited faint grain boundaries (Figure 3f). However, severe corrosion and significant pits were observed on the electrode. This suggests an acceleration of the HER, supported by the substantial formation of bubbles when the metal was placed in the excessive electrolyte solution (Figure S18). On the other hand, bubble formation was significantly suppressed in pectin solution, despite having the same pH as the ZS-H_2SO_4 electrolyte (Figure S19).

To examine the suppression capability of the pectin solution for HER, linear sweep voltammetry (LSV) tests were conducted using a three-electrode cell with carbon paper serving as both the working and counter electrodes. This cell configuration allows the observation of HER separately from the Zn plating reaction.[30a] The LSV curves exhibited a higher current density at the same voltage level and a steeper slope at a higher voltage in the ZS electrolyte compared to those in the ZSP electrolyte, indicating that the pectin as an additive effectively suppresses the HER (Figure S20). Fourier transform infrared (FTIR) spectroscopy was employed to analyze how to affect the pectin to the solvation sheath of Zn^{2+} and the inhibition of HER in electrolyte. The FTIR spectrum exhibited peak intensity

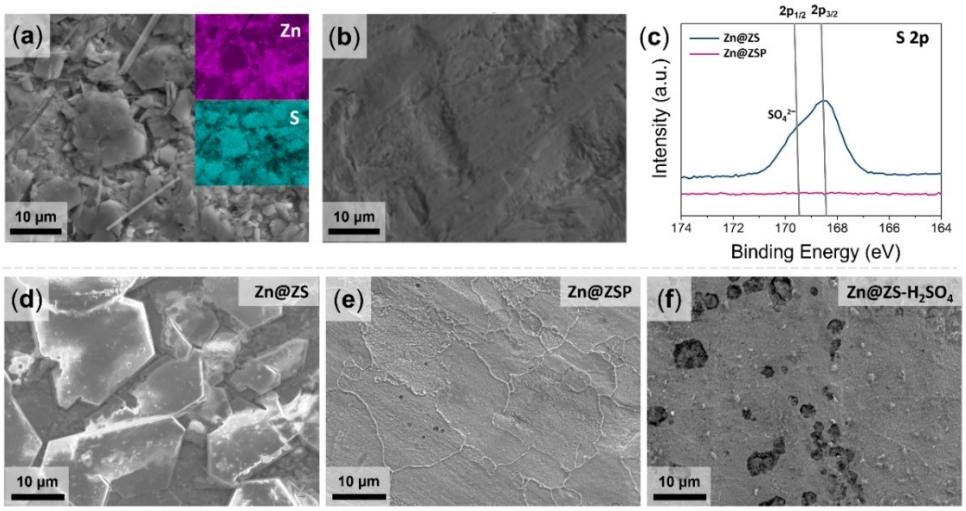

Figure 3. SEM and EDS mapping images of Zn electrode with 100 μL of a) ZS electrolyte and b) ZSP electrolyte after two days. c) S 2p X-ray photoelectron spectra of Zn@ZS and Zn@ZSP electrodes. SEM images of Zn electrode with 10 mL of d) ZS electrolyte (Zn@ZS), e) ZSP electrolyte (Zn@ZSP), and ZS-H_2SO_4 electrolyte (Zn@ZS-H_2SO_4).

© 2024 Wiley-VCH GmbH

Research Article
doi.org/10.1002/batt.202400365
Chemistry Europe
European Chemical Societies Publishing

weakening and positive shift of the O–H stretching peak within the region from 3000 to 3800 cm^{-1} and S–O stretching peak within the region from 800 to 1200 cm^{-1} as introducing pectin, evidencing reduced free water molecules in the ZSP electrolyte and suppressed H_2 evolution (Figure S21).[46] Pectin has water uptake ability and may interact with water molecules in electrolyte, which interrupt and reconstruct the hydrogen bonding network in the electrolyte system.[47] The electrochemical properties of Zn@ZS and Zn@ZSP electrodes were examined using Zn asymmetric and symmetric cells with 3 m $Zn(CF_3SO_3)_2$ electrolyte (Figures 4a, b). Both configuration cells with Zn@ZS exhibited increased polarizations and nucleation overpotentials in compared to the cells with bare Zn due to the ZHS particles accumulated on the surface of Zn. On the other hand, both configuration cells with Zn@ZSP exhibited the lowest polarizations and nucleation overpotentials. Especially in the Zn||Cu cells, the nucleation overpotential with Zn@ZSP was notably lower at 53 mV compared to that with Zn@ZS (104 mV).

The full cells with V_2O_5 cathodes, incorporating Zn electrodes treated with different solutions, were prepared to verify the reversibility of Zn electrodes in AZIBs. We observed that the full cell with bare Zn demonstrated a reasonable capacity retention of 87.2% after 100 cycles and experienced failure at the 215th cycle at 1 A g^{-1}. However, the cell with vanadium-based cathode experienced significant capacity decay at low current density due to the side reactions related to vanadium dissolution,[48] resulting in cell failure at the 128th cycle at 200 mA g^{-1} (Figure S22). To address the practical aspect of high current density and focus on the surface condition of the Zn electrode, the electrochemical test was conducted at 1 A g^{-1} after five activation cycles at 20 mA g^{-1}. During the activation cycles, we observed an increase in specific capacity by comparing the voltage profiles of the first and fifth cycles, consistent with reports that V_2O_5 requires long activation cycles.[49] The first discharge capacity of Zn@ZSP full cell was 228.8 mA h g^{-1}, whereas that of the Zn@ZS cell was 215.4 mA h g^{-1} at 20 mA g^{-1}. As the cycles progressed, the Zn@ZSP cell achieved a capacity of 498.8 mA h g^{-1}, while the Zn@ZS cell reached 469.8 mA h g^{-1} by the fifth cycle (Figure 4c). Moreover, the difference in charge/discharge overpotential increased as the cycle progressed. After activation cycles, the full cell with Zn@ZS failed at the 33rd. The full cell with bare Zn also showed a rapid decrease in capacity and cell failure at the 215th cycle (Figure S22). In contrast, the Zn@ZSP cell demonstrated stable operation without cell failure over 400 cycles at 1 A g^{-1} (Figure 4d).

The improved electrochemical performance might be due to the removal of uneven layer on metallic Zn, the absence of ZHS agglomerates, and the improved wettability to electrolyte. With a ZS electrolyte droplet, a lower contact angle of 78° was observed in Zn@ZS electrode, compared to pristine Zn electrode (99°), owing to the hydrophilic nature of the ZHS particles (Figure 4e top).[31] On the other hand, the contact angle on the Zn@ZSP electrode of 63° was the lowest, indicating superior electrolyte wettability and high affinity between Zn electrode and electrolyte despite the absence of hydrophilic ZHS layer (Figure 4e bottom). Moreover, after immersing Zn@ZSP electrode in excessive ZS for two days, it can be noted that ZHS formation is significantly suppressed compared to bare Zn in the same condition (Figure 4f).

Further, the full cell with different cathode material, manganese dioxide (MnO_2), was used to test the ZHS inhibition effect of Zn@ZSP electrode. The coin cell with synthesized MnO_2 in 3 M $ZnSO_4$ with 0.1 M $MnSO_4$ electrolyte showed reasonable specific capacity at 0.1 A g^{-1} (Figure S23).[50] Firstly, we confirmed the charge transfer resistances in the EIS spectra at different resting time according to anode materials in ZS electrolyte (Figure S24). The MnO_2 full cell with Zn@ZS demon-

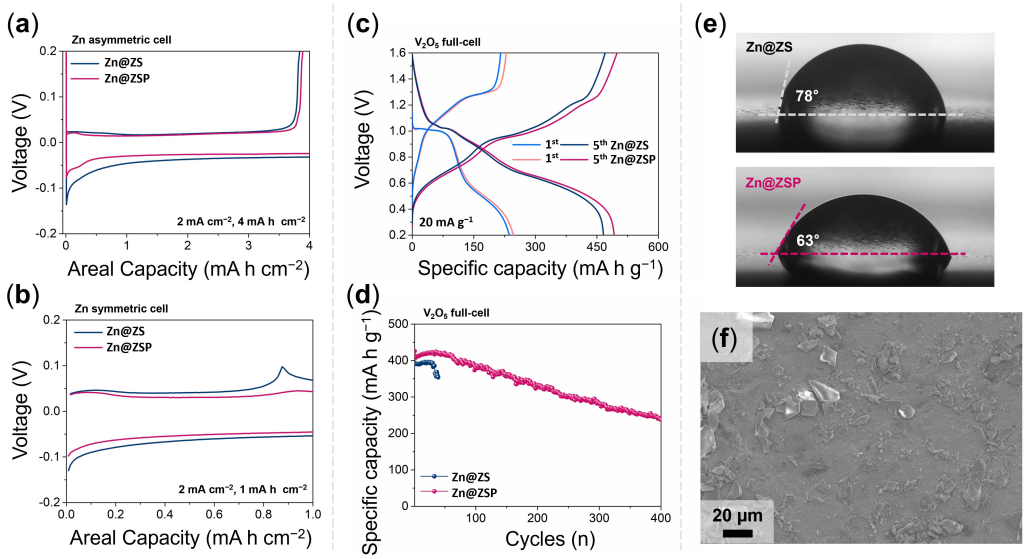

Figure 4. Voltage-time profiles of a) Zn||Cu cells and b) Zn symmetric cells with Zn@ZS and Zn@ZSP electrodes in the first cycle. c) Galvanostatic charge/discharge curves of the V_2O_5||Zn@ZS and V_2O_5||Zn@ZSP full cells at 20 mA g^{-1}. d) Cyclic performance of the V_2O_5||Zn@ZS and V_2O_5||Zn@ZSP full cells at 1 A g^{-1}. e) The contact angles of the droplets of ZS electrolyte on Zn@ZS and Zn@ZSP electrodes. f) SEM images of Zn@ZSP electrode with 10 mL of ZS electrolyte.

© 2024 Wiley-VCH GmbH

25666223, 2024, 12, Downloaded from https://chemistry-europe.onlinelibrary.wiley.com/doi/10.1002/batt.202400365 by University of Ulsan, Wiley Online Library on [11/11/2025]. See the Terms and Conditions (https://onlinelibrary.wiley.com/terms-and-conditions) on Wiley Online Library for rules of use; OA articles are governed by the applicable Creative Commons License

strated a higher charge transfer resistance than that of Zn@ZSP due to the presence of the ZHS particles after two hours of cell assembly. After ten hours, sufficient time for wetting the electrodes in the electrolyte, the EIS spectra of the Zn@ZS cell showed a highly increased charge transfer resistance, while the charge transfer resistance of the cell with Zn@ZSP electrode was almost unchanged. In addition, after five formation cycles at 20 mA g^{-1}, the charge transfer resistance of the Zn@ZSP cell was smaller than that of Zn@ZS cell (Figure S25). Furthermore, the MnO_2 full cell with Zn@ZS electrode and ZS electrolyte experienced failure after 37 cycles, similar to the result observed in the V_2O_5 full cell (Figure S26). In contrast, Zn@ZSP cell with ZS electrolyte after 55 cycles, the similar charge transfer resistance with that of after five formation cycles was observed. Moreover, the MnO_2 cell combining Zn@ZSP electrode and ZSP electrolyte showed the best capacity retention (Figure S27).

Based on the discussed results, the effects of pectin can be summarized as follows: The uneven Zn surface with ZS electrolyte not only accelerates side reactions such as ZHS formation and HER but also allows dendritic Zn to grow due to the uneven Zn^{2+} flux. (Scheme 1 top).[51] Conversely, i) the acidic electrolyte with pectin as an additive inhibits the side reactions and induces the uniform deposition, thereby enhancing the reversibility of the AZIBs (Scheme 1 bottom). ii) As component for the pretreatment solution, submerging in the pectin-based solution exposes a smooth surface by removing the rugged layer on the Zn foil surface. The modified Zn electrode in pectin solution results in the inhibition of ZHS formation and reduced overpotentials.

3. Conclusions

In summary, this study revealed the role of pectin in $ZnSO_4$ electrolyte as i) additive and ii) metal pretreatment solution for AZIBs. In particular, the ZSP electrolyte is effective to prevent the formation of ZHS and suppress HER, thereby enhancing the reversibility of the AZIBs. The Zn asymmetric configuration cell with ZSP exhibited stable cycling for more than 23 times longer than the cell containing ZS at 1 mA cm^{-2} with a deposition capacity of 1 mA h cm^{-2}. Moreover, we found that ZSP has ability to remove the bumpy layer cleanly and reveal the underlying polycrystalline morphology of metallic Zn. The galvanostatic cycling tests in a full cell with V_2O_5 cathode and surface-modified Zn, obtained through immersion in ZSP, demonstrated reduced internal resistance and significantly improved cycle stability without failure for up to 400 cycles at 1 A g^{-1}. Particularly noteworthy is the effective removal of the rough-textured surface layer using an acidic pectin electrolyte. These results provide insights into the potential for acidic solutions containing high-molecular-weight carbohydrate polymer as pretreatment solutions. Moreover, this strategy highlights the possibility of introducing organic acid materials into electrolyte that influence the surface morphology and reversibility of Zn anodes, enhancing the performance of Zn metal anodes for AZIB applications.

Experimental Section

Materials

Pectin from citrus peel was purchased from Sigma-Aldrich. Zinc sulfate heptahydrate ($ZnSO_4 \cdot 7H_2O$, 99.0–103.0%) was purchased from Alfa Aesar. All powders were used without further purification. Deionized water (DI-water) was purified by a HIQ III water purifier.

Characterizations

Scanning electron microscopy (SEM, JEOL JSM-7401F, JSM-7900F) was used to investigate the surface morphologies. Elements of ZHS byproducts were measured by using an energy dispersive spectro-

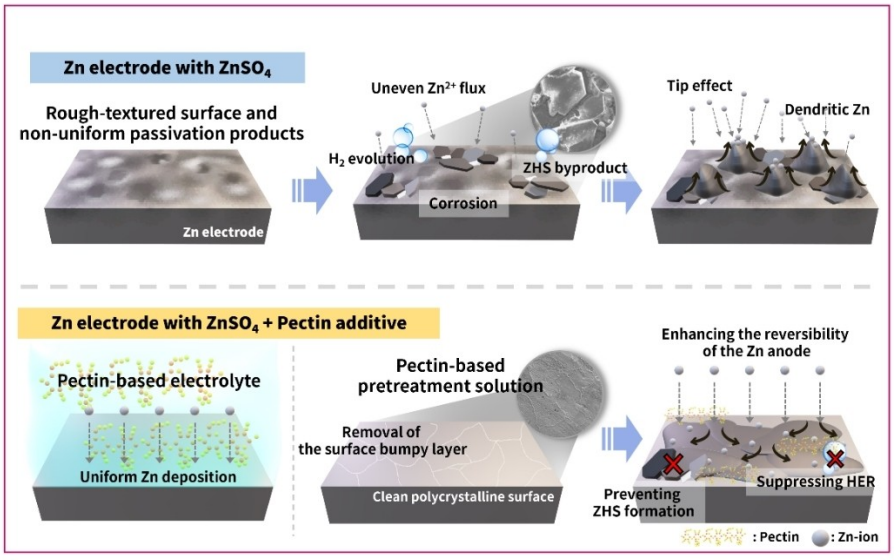

Scheme 1. Schematic illustration of the effects of ZS and acidic pectin-based ZSP electrolyte on Zn electrode.

© 2024 Wiley-VCH GmbH

25666223, 2024, 12, Downloaded from https://chemistry-europe.onlinelibrary.wiley.com/doi/10.1002/batt.202400365 by University of Ulsan, Wiley Online Library on [11/11/2025]. See the Terms and Conditions (https://onlinelibrary.wiley.com/terms-and-conditions) on Wiley Online Library for rules of use; OA articles are governed by the applicable Creative Commons License

scopy (EDS) analysis. Structural information was obtained using an X-ray diffractometer (XRD, D8-Advance Davinci) with Cu Kα radiation in the 2θ range of 20–80°. X-ray photoelectron spectroscopy (XPS, Thermo Scientific ESCALAB 250) was used to determine the chemical composition of the samples. Fourier transform infrared (FTIR) spectroscopy (Perkin Elmer Model Spectrum Two) was used to determine the functional groups and the chemical interactions on the electrolytes. The pH value of electrolytes was obtained by pH meter (Thermo Scientific Orion Star A211 pH benchtop meter).

Electrochemical Characterization

CR2032-type coin cells were assembled for the electrochemical tests. Zn anodes were prepared by cutting a circular disk with a diameter of 16 mm and GF/A was used as the separator. The electrolyte consisted of 1 M $ZnSO_4$ dissolved in DI water as the base electrolyte. Pectin was added to the electrolyte at 0.5, 1.5, 5, 7.5, and 10 wt% relative to the mass of electrolyte salt. 100 μL of electrolyte added into the cell before the cell was crimped. For the pretreatment of the Zn metal surface, the Zn metal was immersed in 10 mL of the solutions for two days. After immersion, the Zn metal was washed several times with water and ethanol. All the electrochemical tests were performed using a WBCS3000 L (WonAtech) cell test system.

Electrochemical impedance spectroscopy (EIS) test was used to measure ionic conductivity (σ) from Nyquist plot. The cell was composed with two titanium (Ti) foil, GF/A as separator, and electrolyte. Impedance measurements were carried out between 10 kHz to 0.02 Hz with an AC amplitude of 10 mV using a ZIVE MP1 (WonAtech Co., Korea) workstation. The equation of ionic conductivity can be expressed as $\sigma = l/R_bA$, where σ is conductivity, and l, R_b, and A represent the separator thickness, the bulk resistance, and the electrode area, respectively.

To investigate the Zn plating/stripping behavior, Zn || Cu asymmetric and Zn symmetric cells were fabricated and tested with various current densities and areal capacities. For rate test, Zn symmetric cells were tested with capacity of 1 mA h cm^{-2} with different current densities (0.5, 1, 2, 5, and 10 mA cm^{-2}) for each 10 cycles.

For ex situ SEM analysis of Zn electrodes, the Zn || Cu asymmetric cells were fabricated and tested with varying current densities and areal capacities. After Zn stripping and plating process, the electrodes were treated as follows: The cycled coin cell was disassembled, and the electrode was rinsed with DI water three times and dried. Subsequently, the electrode was attached to the SEM mount using carbon tape, and top-view SEM images were obtained.

To observe initial stripping morphologies, the Zn || Cu cells were passed through a single stripping process at a current density of 2 mA cm^{-2} with 2 mA h cm^{-2}. The deposition morphology after stripping process were examined using Zn || Cu cells that had undergone the initial stripping process at a current density of 2 mA cm^{-2} with 4 mA h cm^{-2}, followed by plating (deposition) process with varying time and voltage conditions (after 1 min, 1 h, and reaching the voltage at 0.2 V). Moreover, Zn || Cu cells were tested for five cycles to determine the Zn deposition behavior under the influence of glass fiber membrane at deep cycling of 2 mA cm^{-2} with 4 mA h cm^{-2}.

For full-cell tests with pretreated Zn electrode, the vanadium pentoxide (V_2O_5), purchased from Sigma-Aldrich, electrode slurry was made by homogeneously mixing the active materials (V_2O_5), poly(vinylidene fluoride) (PVDF) binder and conductive material (Super C) in the mass ratio of 7:2:1. The area mass loading for the V_2O_5 cathode electrode was ~5 mg cm^{-2}. Thereafter, the slurry was coated on titanium foil, and then vacuum-dried at 100 °C for 12 h.

For full-cell tests with ZSP, the manganese oxide (MnO_2) was used as active materials. α-MnO_2 was synthesized use in a typical synthesis of procedure. 0.512 g $MnSO_4{\cdot}H_2O$ (SAMCHUN, 98%) was dissolved in 20 mL DI water and subsequently, 0.3 g $KMnO_4$ (DAEJUNG, 99.3%) was gradually put into the above obtained solution for with vigorous stirring for 30 min. The mixture was transferred to 25 mL Teflon-lined autoclaves and heated at 160 °C for 20 h. The reaction products were washed by centrifugation with deionized water and ethanol following by dried at 80 °C in vacuum for 12 h. Electrode slurry was made by homogeneously mixing the active materials(α-MnO_2), CMC and SBR binder and conductive material (Super C) in the mass ratio of 7:2:1. The area mass loading for the MnO_2 cathode electrode was 2~3 mg cm^{-2}. Thereafter, the slurry was coated on titanium foil, and then vacuum-dried at 100 °C for 12 h.

Acknowledgements

This work was supported by National Research Foundation of Korea(NRF) grant funded by the Korea government(MSIT) (No. RS-2024–00429941); and by ′ regional innovation mega project′ program through the Korea Innovation Foundation funded by Ministry of Science and ICT (Project Number: 2023-DD-UP-0032).

Conflict of Interests

The authors declare no conflict of interest.

Data Availability Statement

The data that support the findings of this study are available from the corresponding author upon reasonable request.

Keywords: Zn anode · Acidic electrolyte · Electrolyte additive · Surface pretreatment · Aqueous zinc ion battery

[1] a) G. Fang, J. Zhou, A. Pan, S. Liang, *ACS Energy Lett.* **2018**, *3*, 2480–2501; b) W. Kang, C. Jo, *Ceramist* **2021**, *24*, 35–53.
[2] a) X. Zeng, J. Hao, Z. Wang, J. Mao, Z. Guo, *Energy Stor. Mater.* **2019**, *20*, 410–437; b) L. Yuan, J. Hao, C.-C. Kao, C. Wu, H.-K. Liu, S.-X. Dou, S.-Z. Qiao, *Energy Environ. Sci.* **2021**, *14*, 5669–5689; c) J. Lee, J. Yoon, J. Jeon, Y. Hong, S.-G. Oh, H. Huh, *Korean J. Chem. Eng.* **2023**, *40*, 1901–1911.
[3] a) Y. Lv, Y. Xiao, L. Ma, C. Zhi, S. Chen, *Adv. Mater.* **2022**, *34*, 2106409; b) H. Jia, Z. Wang, B. Tawiah, Y. Wang, C.-Y. Chan, B. Fei, F. Pan, *Nano Energy* **2020**, *70*, 104523; c) W. Kang, I. Nam, C. Jo, *Korean J. Chem. Eng.* **2023**, *40*, 1353–1359.
[4] A. Konarov, N. Voronina, J. H. Jo, Z. Bakenov, Y.-K. Sun, S.-T. Myung, *ACS Energy Lett.* **2018**, *3*, 2620–2640.
[5] a) N. Wang, H. Wan, J. Duan, X. Wang, L. Tao, J. Zhang, H. Wang, *Mater. Today Adv.* **2021**, *11*, 100149; b) W. Shang, W. Yu, Y. Liu, R. Li, Y. Dai, C. Cheng, P. Tan, M. Ni, *Energy Stor. Mater.* **2020**, *31*, 44–57; c) W. Zhang, Y. Dai, R. Chen, Z. Xu, J. Li, W. Zong, H. Li, Z. Li, Z. Zhang, J. Zhu, F. Guo, X. Gao, Z. Du, J. Chen, T. Wang, G. He, I. P. Parkin, *Angew. Chem. Int. Ed.* **2023**, *62*, e202212695.
[6] T. Shoji, M. Hishinuma, T. Yamamoto, *J. Appl. Electrochem.* **1988**, *18*, 521–526.
[7] M. Li, Z. Li, X. Wang, J. Meng, X. Liu, B. Wu, C. Han, L. Mai, *Energy Environ. Sci.* **2021**, *14*, 3796–3839.
[8] a) J. Hao, B. Li, X. Li, X. Zeng, S. Zhang, F. Yang, S. Liu, D. Li, C. Wu, Z. Guo, *Adv. Mater.* **2020**, *32*, 2003021; b) W.-G. Lim, X. Li, D. Reed.

© 2024 Wiley-VCH GmbH

25666223, 2024, 12, Downloaded from https://chemistry-europe.onlinelibrary.wiley.com/doi/10.1002/batt.202400365 by University of Ulsan, Wiley Online Library on [11/11/2025]. See the Terms and Conditions (https://onlinelibrary.wiley.com/terms-and-conditions) on Wiley Online Library for rules of use; OA articles are governed by the applicable Creative Commons License

[9] J. Hao, X. Li, S. Zhang, F. Yang, X. Zeng, S. Zhang, G. Bo, C. Wang, Z. Guo, *Adv. Funct. Mater.* **2020**, *30*, 2001263.
[10] a) X. Huang, X. Liu, H. Li, Q. Zhao, T. Ma, *Small Structures* **2023**, *4*, 2200221; b) J. Huang, Z. Wang, M. Hou, X. Dong, Y. Liu, Y. Wang, Y. Xia, *Nat. Commun.* **2018**, *9*, 2906.
[11] D. Reber, R.-S. Kühnel, C. Battaglia, *ACS Mater. Lett.* **2019**, *1*, 44–51.
[12] a) Y. Pan, Z. Liu, S. Liu, L. Qin, Y. Yang, M. Zhou, Y. Sun, X. Cao, S. Liang, G. Fang, *Adv. Energy Mater.* **2023**, *13*, 2203766; b) J. Cao, D. Zhang, R. Chanajaree, Y. Yue, Z. Zeng, X. Zhang, J. Qin, *APM* **2022**, *1*, 100007.
[13] a) Y. Hao, C. Huang, Y. Yang, Y. Qian, G. Chang, Y. Zhang, A. Hu, Q. Tang, X. Chen, *J. Power Sources* **2023**, *584*, 233631; b) X. Feng, P. Li, J. Yin, Z. Gan, Y. Gao, M. Li, Y. Cheng, X. Xu, Y. Su, S. Ding, *ACS Energy Lett.* **2023**, *8*, 1192–1200; c) A. Pomberger, A. A. Pedrina McCarthy, A. Khan, S. Sung, C. J. Taylor, M. J. Gaunt, L. Colwell, D. Walz, A. A. Lapkin, *React. Chem. Eng.* **2022**, *7*, 1368–1379.
[14] Z. Zeng, Y. Zeng, L. Sun, H. Mi, L. Deng, P. Zhang, X. Ren, Y. Li, *Nanoscale* **2021**, *13*, 12223–12232.
[15] X. Zhao, X. Zhang, N. Dong, M. Yan, F. Zhang, K. Mochizuki, H. Pan, *Small* **2022**, *18*, 2200742.
[16] a) E. Xiang, M. N. Gómez-Cerezo, Y. Ali, S. S. Ramachandra, N. Yang, M. Dargusch, C. S. Moran, S. Ivanovski, A. Abdal-hay, *ACS Appl. Mater. Interfaces* **2022**, *14*, 22554–22569; b) E. Xiang, C. S. Moran, S. Ivanovski, A. Abdal-Hay, *Nanomater.* **2023**, *13*, 2022.
[17] W. Wang, G. Huang, Y. Wang, Z. Cao, L. Cavallo, M. N. Hedhili, H. N. Alshareef, *Adv. Energy Mater.* **2022**, *12*, 2102797.
[18] a) E. Lizundia, D. Kundu, *Adv. Funct. Mater.* **2021**, *31*, 2005646; b) J. Jeong, J. Lee, J. Kim, J. Chun, D. Kang, S. M. Han, C. Jo, J. Lee, *J. Mater. Chem. A* **2021**, *9*, 7774–7781; c) J. Jang, J. Oh, H. Jeong, W. Kang, C. Jo, *Materials* **2020**, *13*, 4625.
[19] a) J. Liu, Q. Zhang, T. Zhang, J.-T. Li, L. Huang, S.-G. Sun, *Adv. Funct. Mater.* **2015**, *25*, 3599–3605; b) C. Senthil, S.-S. Kim, H. Y. Jung, *Nat. Commun.* **2022**, *13*, 145; c) Y.-P. Chuang, J.-L. Hong, *ACS Appl. Energy Mater.* **2021**, *4*, 10213–10221.
[20] a) T. Xu, K. Liu, N. Sheng, M. Zhang, W. Liu, H. Liu, L. Dai, X. Zhang, C. Si, H. Du, K. Zhang, *Energy Stor. Mater.* **2022**, *48*, 244–262; b) N. Mittal, S. Tien, E. Lizundia, M. Niederberger, *Small* **2022**, *18*, 2107183; c) C. Fu, Y. Wang, C. Lu, S. Zhou, Q. He, Y. Hu, M. Feng, Y. Wan, J. Lin, Y. Zhang, A. Pan, *Energy Stor. Mater.* **2022**, *51*, 588–598.
[21] a) C. Rolin, *in Industrial Gums (Third Edition)* (Eds: R. L. Whistler, J. N. Bemiller), Academic Press, London, **1993**, 257–293; b) Y. Gomravi, A. Karimi, H. Azimi, *Korean J. Chem. Eng.* **2021**, *38*, 1843–1858.
[22] J. DeRuiter, *Principles of drug action* **2005**, *1*, 1–10.
[23] a) D. Mohnen, *Curr. Opin. Plant Biol.* **2008**, *11*, 266–277; b) C. Lara-Espinoza, E. Carvajal-Millán, R. Balandrán-Quintana, Y. López-Franco, A. Rascón-Chu, *Molecules* **2018**, *23*, 942.
[24] Z. K. Mukhiddinov, D. K. Khalikov, F. T. Abdusamiev, C. C. Avloev, *Talanta* **2000**, *53*, 171–176.
[25] T. O. M. Brody, *in Nutritional Biochemistry (Second Edition)* (Ed: T. O. M. Brody), Academic Press, San Diego, **1999**, pp. 1–56.
[26] a) Z. Jia, W. Zhao, S. Hu, X. Yang, T. He, X. Sun, *ChemComm* **2022**, *58*, 8504–8507; b) Y. Tian, S. Chen, Q. Chen, S. Ding, K. S. Hui, J. Zhang, *Next Energy* **2023**, *1*, 100048; c) Z. Luo, Y. Xia, S. Chen, X. Wu, R. Zeng, X. Zhang, H. Pan, M. Yan, T. Shi, K. Tao, B. B. Xu, Y. Jiang, *Nanomicro Lett.* **2023**, *15*, 205.
[27] N. Zhang, F. Cheng, Y. Liu, Q. Zhao, K. Lei, C. Chen, X. Liu, J. Chen, *J. Am. Chem. Soc.* **2016**, *138*, 12894–12901.
[28] a) Z. X. Lim, K. Y. Cheong, *Phys. Chem. Chem. Phys.* **2015**, *17*, 26833–26853; b) T. Toniazzo, J. P. Fabi, *Fluids* **2023**, *8*, 243.
[29] Q. He, G. Fang, Z. Chang, Y. Zhang, S. Zhou, M. Zhou, S. Chai, Y. Zhong, G. Cao, S. Liang, A. Pan, *Nanomicro Lett.* **2022**, *14*, 93.
[30] a) S.-H. Huh, Y. J. Choi, S. H. Kim, J.-S. Bae, S.-H. Lee, S.-H. Yu, *J. Mater. Chem. A* **2023**, *11*, 19384–19395; b) F.-N. Jiang, S.-J. Yang, H. Liu, X.-B. Cheng, L. Liu, R. Xiang, Q. Zhang, S. Kaskel, J.-Q. Huang, *SusMat* **2021**, *1*, 506–536.
[31] Y.-H. Lee, Y. Jeoun, S.-H. Lee, J. H. Kim, S.-Y. Kim, S.-H. Yu, K.-S. Ahn, Y.-E. Sung, *Chem. Eng. J.* **2023**, *464*, 142580.
[32] S. Di, X. Nie, G. Ma, W. Yuan, Y. Wang, Y. Liu, S. Shen, N. Zhang, *Energy Stor. Mater.* **2021**, *43*, 375–382.
[33] D. Grujicic, B. Pesic, *Electrochim. Acta* **2002**, *47*, 2901–2912.
[34] C. Xie, Y. Li, Q. Wang, D. Sun, Y. Tang, H. Wang, *Carbon Energy* **2020**, *2*, 540–560.
[35] Y.-F. Hu, L.-F. Zhou, H. Gong, H. Jia, P. Chen, Y.-S. Wang, L.-Y. Liu, T. Du, *Korean J. Chem. Eng.* **2022**, *39*, 2353–2360.
[36] a) P. Xiong, Y. Kang, N. Yao, X. Chen, H. Mao, W.-S. Jang, D. M. Halat, Z.-H. Fu, M.-H. Jung, H. Y. Jeong, Y.-M. Kim, J. A. Reimer, Q. Zhang, H. S. Park, *ACS Energy Lett.* **2023**, *8*, 1613–1625; b) S. H. Park, S. Y. Byeon, J.-H. Park, C. Kim, *ACS Energy Lett.* **2021**, *6*, 3078–3085.
[37] a) A. Mitha, A. Z. Yazdi, M. Ahmed, P. Chen, *ChemElectroChem* **2018**, *5*, 2409–2418; b) D. Kong, Q. Zhang, L. Li, H. Zhao, R. Liu, Z. Guo, L. Wang, *Batteries* **2023**, *9*, 262.
[38] Y. Qin, P. Liu, Q. Zhang, Q. Wang, D. Sun, Y. Tang, Y. Ren, H. Wang, *Small* **2020**, *16*, 2003106.
[39] a) Y. Zhang, G. Yang, M. L. Lehmann, C. Wu, L. Zhao, T. Saito, Y. Liang, J. Nanda, Y. Yao, *Nano Lett.* **2021**, *21*, 10446–10452; b) J. Jang, J. Chun, C. Jo, *Energy Stor. Mater.* **2023**, *62*, 102948.
[40] Y. Zhu, F. Wang, L. Liu, S. Xiao, Y. Yang, Y. Wu, *Sci. Rep.* **2013**, *3*, 3187.
[41] a) P. Chen, X. Yuan, Y. Xia, Y. Zhang, L. Fu, L. Liu, N. Yu, Q. Huang, B. Wang, X. Hu, Y. Wu, T. van Ree, *Adv. Sci.* **2021**, *8*, 2100309; b) D.-Q. Li, J. Li, H.-L. Dong, X. Li, J.-Q. Zhang, S. Ramaswamy, F. Xu, *Int. J. Biol. Macromol.* **2021**, *185*, 49–65.
[42] G. Li, Z. Zhao, S. Zhang, L. Sun, M. Li, J. A. Yuwono, J. Mao, J. Hao, J. Vongsvivut, L. Xing, C.-X. Zhao, Z. Guo, *Nat. Commun.* **2023**, *14*, 6526.
[43] Y. Shao, Z. Sun, Z. Tian, S. Li, G. Wu, M. Wang, X. Tong, F. Shen, Z. Xia, V. Tung, J. Sun, Y. Shao, *Adv. Funct. Mater.* **2021**, *31*, 2007843.
[44] X. Chen, X. Shi, P. Ruan, Y. Tang, Y. Sun, W.-Y. Wong, B. Lu, J. Zhou, *Small Science* **2023**, *3*, 2300007.
[45] G. Pan, J. Chen, K. Ge, L. Yang, F. Li, Z. Wang, S. Shi, X. Yang, Z. Zhou, A. Tang, W. Liu, Y. Sun, *J. Mater. Chem. C* **2019**, *7*, 4449–4458.
[46] a) F. Yang, J. A. Yuwono, J. Hao, J. Long, L. Yuan, Y. Wang, S. Liu, Y. Fan, S. Zhao, K. Davey, Z. Guo, *Adv. Mater.* **2022**, *34*, 2206754; b) Z. Liu, R. Wang, Q. Ma, J. Wan, S. Zhang, L. Zhang, H. Li, Q. Luo, J. Wu, T. Zhou, J. Mao, L. Zhang, C. Zhang, Z. Guo, *Adv. Funct. Mater.* **2024**, *34*, 2214538; c) J. Hao, L. Yuan, C. Ye, D. Chao, K. Davey, Z. Guo, S.-Z. Qiao, *Angew. Chem. Int. Ed.* **2021**, *60*, 7366–7375.
[47] U. Einhorn-Stoll, *Food Hydrocoll.* **2018**, *78*, 109–119.
[48] X. Dou, X. Xie, S. Liang, G. Fang, *Science Bulletin* **2024**, *69*, 833–845.
[49] a) R. Li, H. Zhang, Q. Zheng, X. Li, *J. Mater. Chem. A* **2020**, *8*, 5186–5193; b) Y. Kim, Y. Park, M. Kim, J. Lee, K. J. Kim, J. W. Choi, *Nat. Commun.* **2022**, *13*, 2371.
[50] H. Pan, Y. Shao, P. Yan, Y. Cheng, K. S. Han, Z. Nie, C. Wang, J. Yang, X. Li, P. Bhattacharya, K. T. Mueller, J. Liu, *Nat. Energy* **2016**, *1*, 16039.
[51] J. Chen, W. Zhao, J. Jiang, X. Zhao, S. Zheng, Z. Pan, X. Yang, *Energy Stor. Mater.* **2023**, *59*, 102767.

Manuscript received: June 4, 2024
Revised manuscript received: July 9, 2024
Accepted manuscript online: July 9, 2024
Version of record online: September 5, 2024

© 2024 Wiley-VCH GmbH

25666223, 2024, 12, Downloaded from https://chemistry-europe.onlinelibrary.wiley.com/doi/10.1002/batt.202400365 by University of Ulsan, Wiley Online Library on [11/11/2025]. See the Terms and Conditions (https://onlinelibrary.wiley.com/terms-and-conditions) on Wiley Online Library for rules of use; OA articles are governed by the applicable Creative Commons License